Egyptian Journal of Radiology and Nuclear Medicine

RESEARCH

Open Access

Diagnostic value of positron emission tomography/computed tomography (PET/CT) in detection of peritoneal carcinomatosis

Ahmed Abdelmonem Darweesh[1*†], Ashraf F. Barakat[2†], Mohamed Fathy Dawoud[1†] and Ekhlas Abdelmonem Shaban[1†]

Abstract

Background The diagnosis of peritoneal carcinomatosis is challenging and can be difficult to detect with imaging, especially the detection of small-sized peritoneal lesions. The presence of peritoneal neoplastic spread alters tumour staging and is one of the most significant prognostic indicators in several malignancies, and the purpose of this study was to highlight the diagnostic value of PET/CT in detection of peritoneal carcinomatosis in patients with malignant neoplastic disease.

Results PET/CT has 76.2% sensitivity, 88.9% specificity, 94.1% PPV, 61.5% NPV and 80% accuracy in detection of peritoneal carcinomatosis. Different patterns of FDG uptake of peritoneal carcinomatosis were found such as focal nodular uptake, diffuse abdominal uptake and liver surface focal or diffuse uptake. From all these different patterns, focal nodular uptake was the most frequent pattern. The best cut-off value of SUVmax was 5 for diagnosis.

Conclusions The study affirms the significant role of PET/CT in the diagnosis of peritoneal carcinomatosis and its important value in the staging, management and follow-up of patients with secondary peritoneal malignancies, especially in case of unavailable or inappropriate peritoneal biopsy. Therefore, PET/CT could help reduce the number of laparotomies and a better selection of patients who are candidates for adjuvant chemotherapy.

Keywords Peritoneal carcinomatosis, Peritoneal metastasis, Omental cake, PET/CT

Background

The peritoneum, omenta and mesenteries are common sites for secondary disease extension from adjacent visceral organs and distant metastatic deposits. Although advances in imaging technology have allowed a significant increase in spatial resolution, the depiction of a peritoneal disease remains a challenge, in part due to its complex anatomical configuration and in part due to the extensive surface area that may host typically small or nodular tumour deposits [1].

The presence of peritoneal neoplastic spread alters tumour staging and is one of the most significant prognostic indicators in several malignancies, especially in ovarian cancer and colorectal carcinoma in which the prognostic significance of peritoneal spread is superior and more powerful for its adverse outcome than tumour extent or lymph node involvement [2–4].

Therefore, early detection and localization is of crucial importance for possible surgical treatment or cytoreductive therapy before surgery [5, 6].

The present study was done to highlight the diagnostic value of positron emission tomography/computed

†Ahmed Abdelmonem Darweesh, Ashraf F. Barakat, Mohamed Fathy Dawoud and Ekhlas Abdelmonem Shaban contributed equally to this work

*Correspondence:
Ahmed Abdelmonem Darweesh
ahmednooman2010@yahoo.com
[1] Department of Radiodiagnosis and Medical Imaging, Faculty of Medicine, Tanta University, Tanta, Egypt
[2] Department of Oncology and Nuclear Medicine, Faculty of Medicine, Tanta University, Tanta, Egypt

tomography (PET/CT) in the detection of peritoneal carcinomatosis in patients with malignant neoplastic disease.

Patients and methods

Patients

A prospective study was carried out on 30 patients (22 females and eight males with ages ranged from 39–85 years and a mean age of 61 ± 11 years) with primary malignant tumours and suspected to have peritoneal carcinomatosis. The study was performed at the PET/CT unit—Diagnostic Radiology and Medical Imaging department, during the period from January 2021 to December 2021. All patients were subjected to the following: Patients' inclusion criteria included: suspected patients known to have a primary malignant tumour, patients with metastasis of unknown primary (MUP) and had incidental peritoneal lesions. Exclusion criteria included patient's age ≤ 18, serum glucose level ≥ 150 mg/dl, serum creatinine ≥ 1.2 mg/dl (normal level) and patients with primary tumours of lymphoma, sarcoma, melanoma and peritoneal mesothelioma. Approval of the Research Ethics Committee and written consent were obtained from all participants in the study. Privacy of all patient data was guaranteed.

Methods

The examination was done using a PET/CT system [Philips Medical Systems-Cleveland-Gemini TF (Time of flight)—USA including a PET scanner combined with a 16 MDCT scanner]. All the patients fasted for at least 6 h prior to the examination. As part of the routine protocol, the patient was injected (18F-FDG) manually intravenously (IV) 60 min before the start of the examination. The dose was calculated with the formula = 3.7 MBq/kgm with a maximum dose = 370 MBq. 0.1 millicurie/kgm (mCi/kg) maximum dose = 10 mCi/kg (18F-FDG). Emptying the urinary bladder is initiated before starting the examination. First, non-contrast low-dose CT images were obtained, and then PET scans from the head to the mid-thighs were acquired followed by routine axial imaging with IV contrast-enhanced CT from the head to mid-thighs at 3-mm intervals. The contrast medium was a non-ionic material, e.g. Iopamidol 300 mgI/ml—and was given at a dose of 1–2 ml/kg at a rate of 3–4 ml/s. The PET/CT scans were done with the following parameters, PET imaging was done in the supine position and whole body scanning was done in 8-bed positions each with an axial field of view of approximately 15 cm/bed position. The CT parameters were: 120 kV, 50 mA, 3 mm slice thickness and 0.5 mm incrimination. The acquisition time of emission data was 1–2 min/bed position in a craniocaudal direction with a total examination time range between 24–38 min.

Image interpretation and analysis

The raw data were reconstructed using special workstations and software. All images were reconstructed in sagittal and coronal multiplanar planes in a video mode on a workstation [Philips-Gemini TF] to get images with a determination of the standard uptake value (SUV) for qualitative and quantitative evaluation interpretation. All PET/CT examinations were analysed separately by a consensus of at least 2 experienced observers of nuclear medicine physicians and radiologists. The maximum uptake value was calculated for every lesion after applying regions of interest (ROI) in the axial attenuation-corrected PET slices. A maximum of SUV more than 5 was considered significant. The malignant lesion is considered if there is a focal increase in the SUV corresponding to the specific location in CT images. A gold standard for all patients in this study depended on the histopathology for the primary tumour and on follow-up (clinical and radiological) or histological type whenever possible for the peritoneal lesions. Lesions were considered positive if showed high FDG uptake by visual assessment. True-positive lesions were considered if the lesions resolved or improved as regards lesion size, number and/or FDG uptake after receiving chemotherapy on follow-up PETCT examination. False-positive lesions were considered if the lesions persisted on follow-up PETCT examination after receiving chemotherapy followed by a negative histopathological assessment. Lesions were considered negative if showed low FDG uptake by visual assessment. True-negative lesions were considered if the lesions persisted as regards lesion size, number and/or FDG uptake on follow-up PETCT examination. False-negative lesions were considered if the lesions showed an increase in FDG uptake on follow-up PETCT examination or showed progression of the disease.

Statistical analysis

The accuracy of PET/CT was expressed in terms of sensitivity, specificity, accuracy and positive and negative predictive values. The difference in accuracy was tested using the Chi-square test. p values less than 0.05 was considered significant. p values more than 0.05 was considered insignificant. Receiver operating characteristic (ROC) curve analysis was performed to evaluate whether SUV-max was able to allow the diagnosis of peritoneal carcinomatosis lesions and to identify the best cut-off value. Statistical calculations were done using computer programs Microsoft Excel 2010 (Microsoft Corporation, NY,

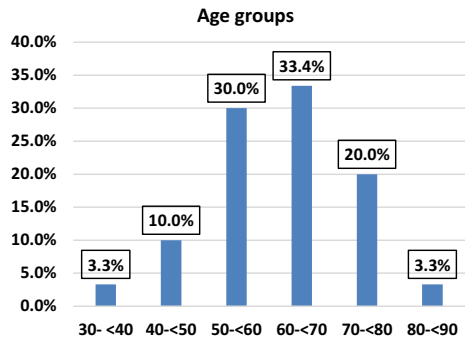

Fig. 1 Column chart showing the distribution of the studied cases according to patients' age

USA) and SPSS software package version 20 (Armonk, NY,USA).

Results

The present study included 30 patients with malignant tumours suspected to have peritoneal carcinomatosis. The study patients included 22 females (73.3%) and 8 males (26.7%) with ages ranged from 39 to 85 years and a mean age of 61.5 ± 11.1 years (Fig. 1).

Different primary tumours were included in this study. The colonic mucinous adenocarcinoma, poorly differentiated gastric adenocarcinoma, ovarian serous cystadenocarcinoma and metastasis of unknown primary (MUP) were the most frequent primary tumours to disseminate to the peritoneum.

Positive patients were 17 based on high FDG uptake by visual assessment in PETCT. True-positive patients were 16 where their lesions resolved or improved as regards lesion size, number and/or FDG uptake after receiving chemotherapy on follow-up PETCT examination. Only one false-positive patient was found where the lesions persisted on follow-up PETCT examination after receiving chemotherapy followed by a negative histopathological assessment. Negative patients were 13 based on low FDG uptake by visual assessment in PETCT. True-negative patients were 8, where their lesions persisted as regards lesion size, number and/or FDG uptake on follow-up PETCT examination. False-negative patients were 5, where their lesions showed increase in FDG uptake on follow-up PETCT examination or showed progression of the disease.

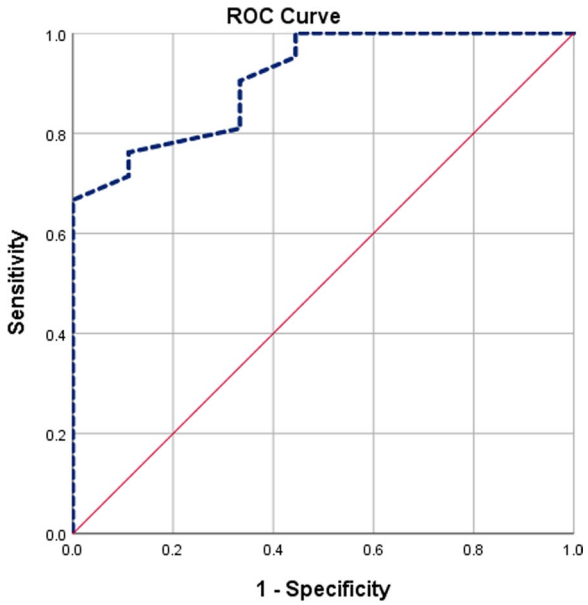

Fig. 2 ROC curve plotted for diagnosis of peritoneal carcinomatosis based on SUVmax

The ROC curve of SUVmax in all included patients is shown in Fig. 2, and the best cut-off value was 5 for the diagnosis of peritoneal carcinomatosis with the area under the curve (AUC) = 0.910 and statistical significance ($p = 0.001$).

The sensitivity was 76.2% and specificity was 88.9%. Positive predictive value (PPV) was (94.1%), the negative predictive value (NPV) was 61.5%, and accuracy was 80.0% (Table 1).

The range of FDG uptake was 1.3–25.0 with a mean SUVmax of FDG uptake = 8.04 ± 6.14. The SUVmax of FDG uptake was found > 5 in 17 patients (56.7%), while was found ≤ 5 in 13 patients (43.3%) (Fig. 3).

Different patterns of FDG uptake of peritoneal carcinomatosis were found as follows: focal nodular uptake was found in 25 patients (51%), diffuse abdominal uptake in 14 patients (28.6%) and liver surface focal or diffuse uptake in ten patients (20.4%) (Fig. 4).

From all these different patterns of FDG uptake of peritoneal carcinomatosis, focal nodular uptake was the most

Table 1 Ability of SUVmax for diagnosis of peritoneal carcinomatosis

	Cut-off	AUC	P	Sensitivity	Specificity	PPV	NPV	Accuracy
SUV max	5.0	0.910	0.001*	76.2%	88.9%	94.1%	61.5%	80.0%

AUC Area Under the Curve; *PPV* Positive predictive value; *NPV* Negative predictive value; *p* probability; *, Significance < 0.05

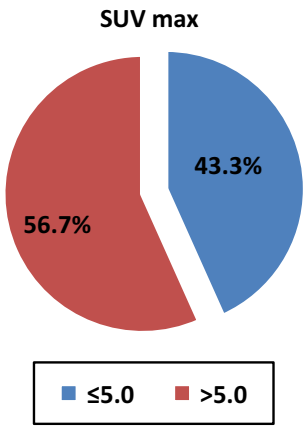

Fig. 3 Pie chart showing the SUVmax for FDG uptake in patients included in the study

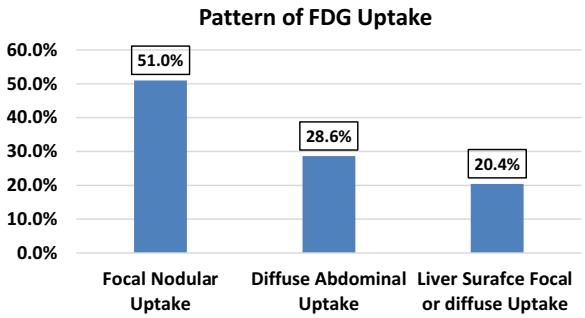

Fig. 4 Column chart showing the distribution of the studied cases according to pattern of FDG uptake

frequent pattern in relation to primary tumours, and there was no significant difference among the patterns (Table 2).

Different sites of peritoneal metastases found in the present study in relation to the primary tumours are shown in Table 3.

From all sites, the greater omentum was the most frequent site of peritoneal metastasis from most of the tumours included in this study in 26 patients (25.7%) ($p=0.180$). The most significantly frequent tumours disseminated to the bowel serosa were the ovarian and colon carcinoma ($p=0.006$) (Tables 4, 5 and Figs. 5, 6, 7 and 8).

Discussion

Peritoneal carcinomatosis (PC) is the intraperitoneal dissemination of any tumour that does not originate from the peritoneum itself. It is the most common diffuse peritoneal disease. Improvement in its diagnosis and treatment affects its prognosis [7].

The present prospective study included 30 patients with malignant tumours suspected to have peritoneal carcinomatosis. The study patients included 22 females (73.3%) and eight males (26.7%) with ages ranged from 39 to 85 years and a mean age of 61.5 ± 11.1 years. In the present study, PETCT was able to diagnose 16 out of 30 patients with sensitivity (76.2%) and specificity (88.9%). The examination showed a positive predictive value (PPV) (94.1%), negative predictive value (NPV) (61.5%) and accuracy (80.0%).

Table 2 Pattern of FDG uptake patients in relation to the primary tumour

Type	Focal Nodular Uptake		Diffuse Abdominal Uptake		Liver Surface Focal or diffuse Uptake		Total[+]	
	n	%	*n*	%	*n*	%	*n*	%
Ovarian	4	16.0	3	21.4	4	40.0	11	22.4
Endometrial	3	12.0	2	14.3	2	20.0	7	14.3
Colon	6	24.0	3	21.4	1	10.0	10	20.4
Gastric	3	12.0	0	0.0	2	20.0	5	10.2
Breast	1	4.0	2	14.3	0	0.0	3	6.1
MUP	1	4.0	2	14.3	1	10.0	4	8.2
Liver	1	4.0	0	0.0	0	0.0	1	2.0
Biliary	1	4.0	0	0.0	0	0.0	1	2.0
Oesophagus	2	8.0	0	0.0	0	0.0	2	4.1
Pancreas	1	4.0	1	7.1	0	0.0	2	4.1
Urinary Bladder	1	4.0	0	0.0	0	0.0	1	2.0
Lung	1	4.0	1	7.1	0	0.0	2	4.1
X^2	**14.640**		**11.116**		**13.650**			
^{MC}p	**0.240**		**0.544**		**0.244**			

Bold indicates X^2: Chi-square test, MC: Monte Carlo exact test

Data expressed as frequency (*n* and %); *MUP* Metastases of unknown primary; [+] Most of the included patients showed more than one pattern of FDG uptake of peritoneal metastasis; *p* probability; Significance < 0.05

Table 3 Sites of malignant peritoneal spread among patients in the present study

Site of peritoneal metastasis	*n*	%
Perihepatic fissures and spaces	7	6.9
Liver and spleen surface	13	12.9
Right subhepatic space	6	5.9
Lesser Omentum	5	5.0
Paracolic gutters	7	6.9
Greater Omentum	26	25.7
Bowel Serosa	23	22.8
Pelvis	9	8.9
Krukenberg	3	3.0
Sister Mary Joseph Nodules	2	2.0
Total	101[+]	100.0

[+] Most of the included patients showed more than one site of peritoneal metastasis

Out of 17 patients included in this study and diagnosed with peritoneal carcinomatosis using PET/CT, 16 patients were true-positive on follow-up. Only one false-positive patient was found after follow-up and negative histopathological examination.

Out of 13 patients included in the present work and excluded to have peritoneal carcinomatosis by PET/CT, on follow-up, eight patients were true-negative and five patients were false-negative.

Soussan et al. [8] were consistent with our findings. The study reported good sensitivity (84%) and specificity (84%) as well as accuracy (80%) for PET/CT in the diagnosis of peritoneal carcinomatosis.

In this study, the range of SUVmax of FDG uptake among all enrolled patients was 1.3–25.0, and the mean SUVmax of FDG uptake was 8.04 ± 6.14. The best cut-off value of SUVmax was 5 for the diagnosis of peritoneal carcinomatosis with statistical significance ($p = 0.001$).

Suzuki et al. [9] also reported that the use of an intra-abdominal FDG uptake cut-off value for SUVmax of > 5.1 assists in the diagnosis of peritoneal carcinomatosis, which is in line with our findings.

In the current study, different patterns of FDG uptake of peritoneal carcinomatosis were found as follows: focal nodular uptake, diffuse abdominal uptake and liver surface focal or diffuse uptake. Moreover, focal nodular uptake was the most frequent pattern seen in 25 patients (51%).

Funicelli et al. [10] found that the [18F] FDG-PET/CT examination showed 47 nodular uptakes (75%) of the 62 nodules reported at surgery; the diffuse uptake pattern was seen in seven scans (70%) of the ten reported at the surgery.

Different primary tumours were included during the study. Colonic mucinous adenocarcinoma, poorly

Table 4 Distribution of studied cases according to the site of peritoneal metastasis related to the primary tumour

Type	Perihepatic fissures and spaces		Liver and spleen surface		Right subhepatic space		Lesser Omentum		Paracolic gutters	
	n	%	*n*	%	*n*	%	*n*	%	*n*	%
Ovarian	1	14.3	3	23.1	1	16.7	0	0.0	2	28.6
Endometrial	2	28.6	2	15.4	0	0.0	1	20.0	0	0.0
Colon	2	28.6	1	7.7	4	66.7	0	0.0	5	71.4
Gastric	1	14.3	2	15.4	0	0.0	1	20.0	0	0.0
Breast	0	0.0	0	0.0	0	0.0	0	0.0	0	0.0
MUP	1	14.3	2	15.4	1	16.7	2	40.0	0	0.0
Liver	0	0.0	1	7.7	0	0.0	1	20.0	0	0.0
Biliary	0	0.0	0	0.0	0	0.0	0	0.0	0	0.0
Oesophagus	0	0.0	0	0.0	0	0.0	0	0.0	0	0.0
Pancreas	0	0.0	1	7.7	0	0.0	0	0.0	0	0.0
Urinary Bladder	0	0.0	1	7.7	0	0.0	0	0.0	0	0.0
Lung	0	0.0	0	0.0	0	0.0	0	0.0	0	0.0
Total[+]	7	100.0	13	100.0	6	100.0	5	100.0	7	100.0
X^2	**6.894**		**13.575**		**12.500**		**15.600**		**18.634**	
^{MC}p	**0.943**		**0.247**		**0.410**		**0.184**		**0.039***	

Bold indicates X^2: Chi-square test, MC: Monte Carlo exact test

Data expressed as frequency (*n* and %); *MUP* Metastases of unknown primary; [+] Most of the included patients showed more than one site of peritoneal metastasis; *p* probability; *, significance < 0.05

Table 5 Distribution of studied cases according to the site of peritoneal metastasis related to the primary tumour

Type	Greater Omentum		Bowel Serosa		Pelvis		Krukenberg		Sister Mary Joseph Nodules	
	n	%	*n*	%	*n*	%	*n*	%	*n*	%
Ovarian	5	19.2	5	21.7	1	11.1	0	0.0	1	50.0
Endometrial	3	11.5	3	13.0	1	11.1	0	0.0	0	0.0
Colon	5	19.2	6	26.1	2	22.2	1	33.3	1	50.0
Gastric	2	7.7	1	4.3	1	11.1	1	33.3	0	0.0
Breast	3	11.5	3	13.0	1	11.1	1	33.3	0	0.0
MUP	3	11.5	2	8.7	0	0.0	0	0.0	0	0.0
Liver	1	3.8	0	0.0	0	0.0	0	0.0	0	0.0
Biliary	1	3.8	0	0.0	0	0.0	0	0.0	0	0.0
Oesophagus	2	7.7	0	0.0	1	11.1	0	0.0	0	0.0
Pancreas	1	3.8	1	4.3	1	11.1	0	0.0	0	0.0
Urinary Bladder	0	0.0	1	4.3	1	11.1	0	0.0	0	0.0
Lung	0	0.0	1	4.3	0	0.0	0	0.0	0	0.0
Total^{+}	26	100.0	23	100.0	9	100.0	3	100.0	2	100.0
X^2	**17.019**		**22.547**		**7.937**		**5.926**		**3.750**	
^{MC}P	**0.180**		**0.006***		**0.874**		**0.915**		**1.000**	

Bold indicates X^2: Chi-square test, MC: Monte Carlo exact test

Data expressed as frequency (*n* and %); *MUP* Metastases of unknown primary; $^{+}$ Most of the included patients showed more than one site of peritoneal metastasis; *p* probability; *, significance < 0.05

differentiated gastric adenocarcinoma, ovarian serous cystadenocarcinoma and MUP were the most frequent primary tumours to disseminate to the peritoneum.

Agreement with other studies like Campos et al. [11] reported that the ovary, colon and stomach are the most frequent sites of origin for secondary peritoneal neoplasms.

Among the studied patients, the greater omentum was the most frequent site of peritoneal metastasis from most of the tumours included.

Patel et al. [1] reported that peritoneal metastases are common within the greater omentum. Moreover, a normal-appearing omentum either on imaging or surgical macroscopic inspection is found to have microscopic peritoneal metastases on histology.

Our study had some limitations. Histological assessment was not performed for all patients. The major drawbacks of PET imaging are its radiation exposure, higher cost and limited depiction of small tumour volumes (current spatial resolution 4 mm) because most of the peritoneal tumour implants are small nodules. Other limitations include the underestimation of uptake due to physiologic movements of the bowel and the normal uptake by the liver, stomach and colon which is sometimes difficult to distinguish from that of peritoneal carcinomatosis.

Conclusions

The present study indicates the significant role of PET/CT in the diagnosis of peritoneal carcinomatosis. This demonstrates its important value in the staging, management and follow-up of patients with secondary peritoneal malignancies, especially in case of unavailable or inappropriate peritoneal biopsy. Therefore, PET/CT may help reduce the number of laparotomies and in a better selection of patients who are candidates for adjuvant chemotherapy.

(See figure on next page.)

Fig. 5 A 72-year-old female patient, investigations revealed increased endometrial thickness, pathologically proved endometrioid endometrial carcinoma, referred for initial staging **A** Axial contrast-enhanced CT. **B** Axial PET slice at the same level. **C** Corresponding axial fused PET/CT image, showing metabolically active omental cake seen as a soft tissue mass underneath anterior abdominal wall (blue arrow), eliciting high focal FDG uptake pattern of SUV max = ~ 11. **D** Axial contrast-enhanced CT. **E** Axial PET slice at the same level. **F** Corresponding axial fused PET/CT image, showing intense endometrial uptake, is seen within the uterus eliciting SUV max = ~ 11. **G** Mid-sagittal PET image showing increased activity underneath the anterior abdominal wall due to omental uptake in addition to increased activity at the uterus (seen above the urinary bladder) (red arrows)

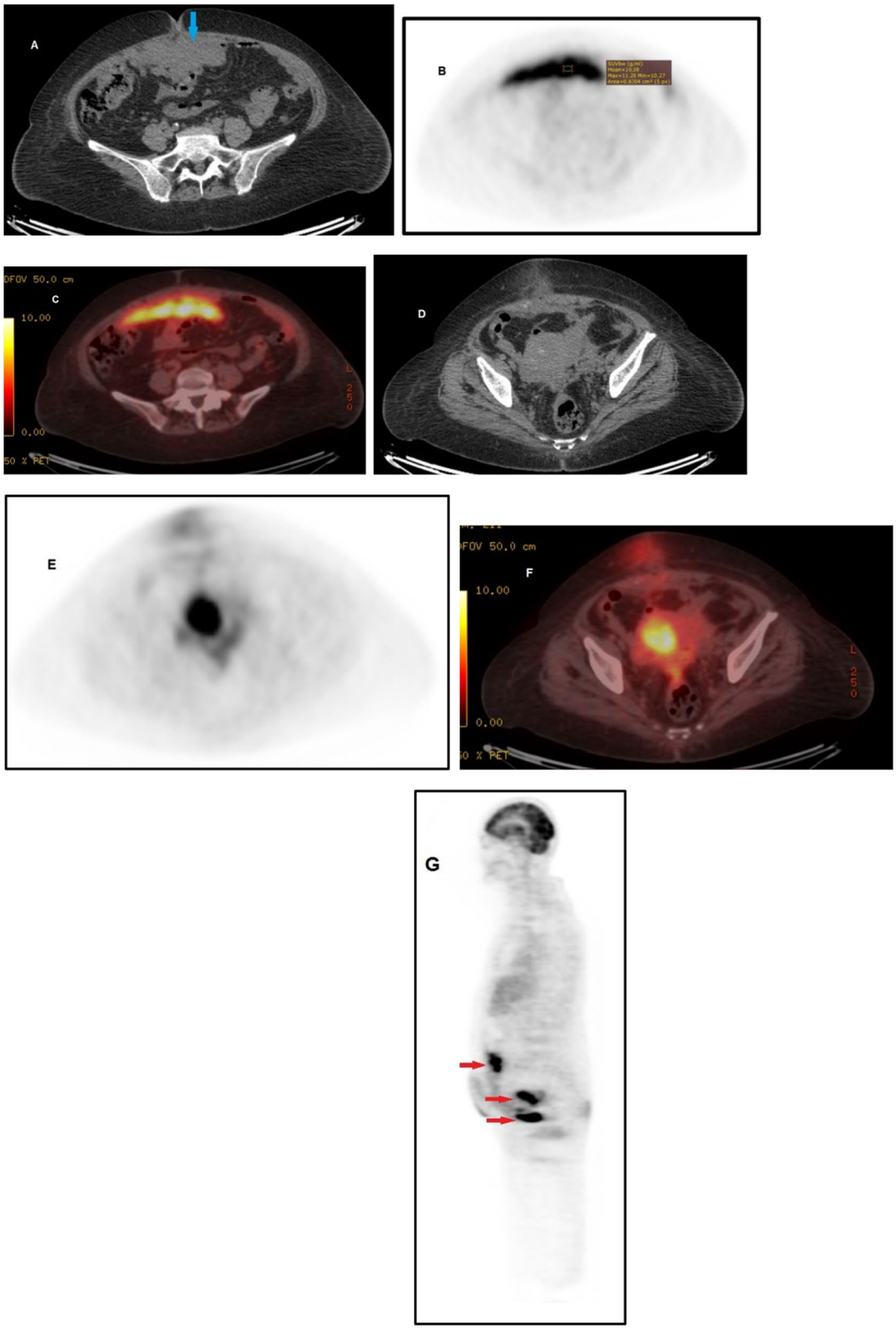

Fig. 5 (See legend on previous page.)

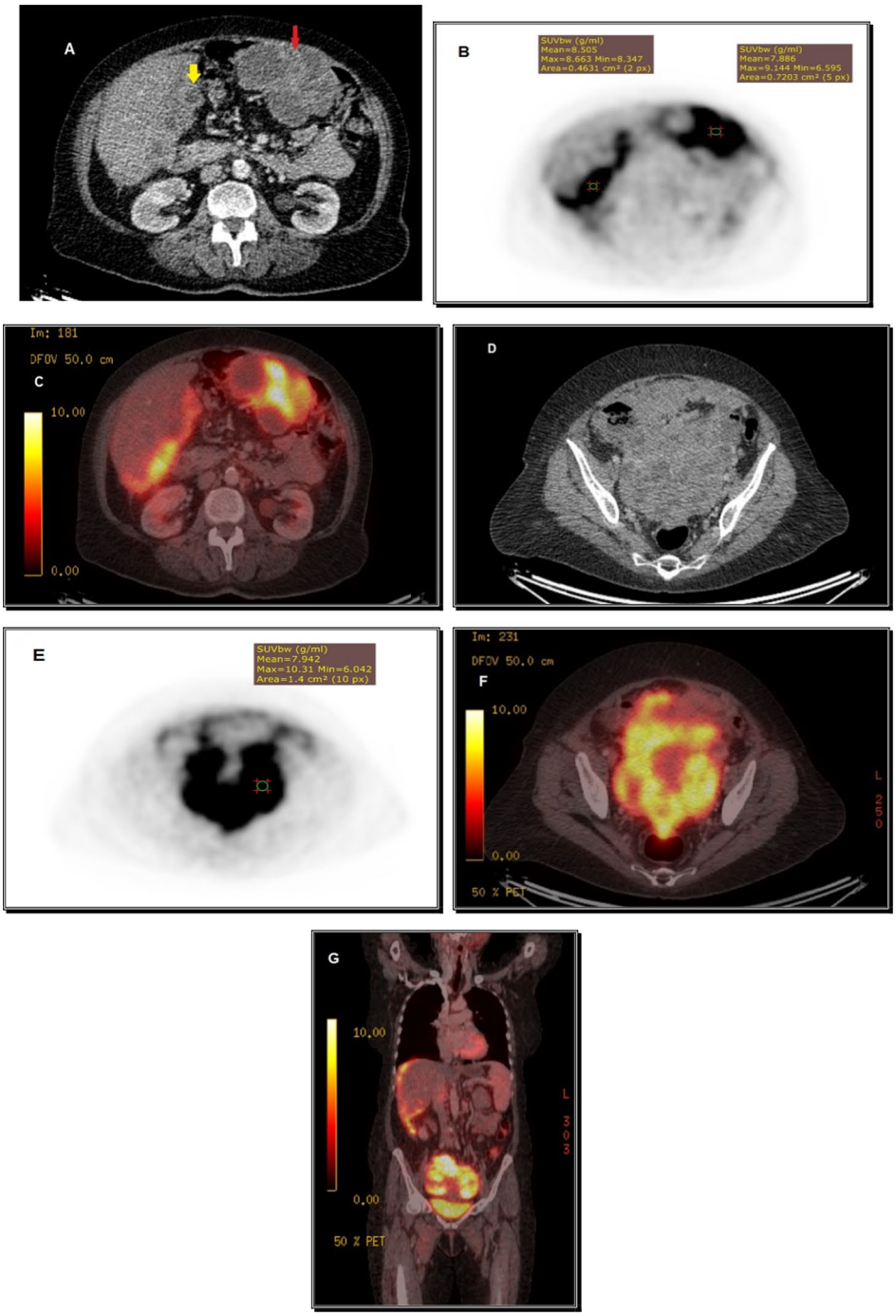

Fig. 6 A 65-year-old female patient with a history of ovarian cancer pathologically proven ovarian mucinous cystadenocarcinoma, referred for whole body survey **A** Axial contrast-enhanced CT. **B** Axial PET slice at the same level. **C** Corresponding axial fused PET/CT image, showing Intense metabolically active multiple hypodense peritoneal nodules creeping along and indenting the inferior and lateral serosal surfaces of the liver, the largest is resting upon the gall bladder fossa (yellow arrow) in addition to left hypochondrial enhancing soft tissue mass lesion showing areas of internal breaking down underneath anterior abdominal wall inseparable from bowel serosa (red arrow), both eliciting SUV max ~ 8.6 and 9.1, respectively. **D** Axial contrast-enhanced CT. **E** Axial PET slice at the same level. **F** Corresponding axial fused PET/CT image, showing bilateral adnexal heterogeneously enhancing large solid mass lesions with areas of breaking down, almost totally occupying the pelvic cavity with significant mass effect upon the surroundings, inseparable from the uterus, posteriorly infiltrating the recto-sigmoid colon and upper rectum and resting upon the urinary bladder, eliciting SUVmax = ~ 10. **G** Coronal PET/CT image demonstrating intense FDG diffuse liver surfaces uptake in addition to the pelvic soft tissue mass lesion seen resting upon the urinary bladder

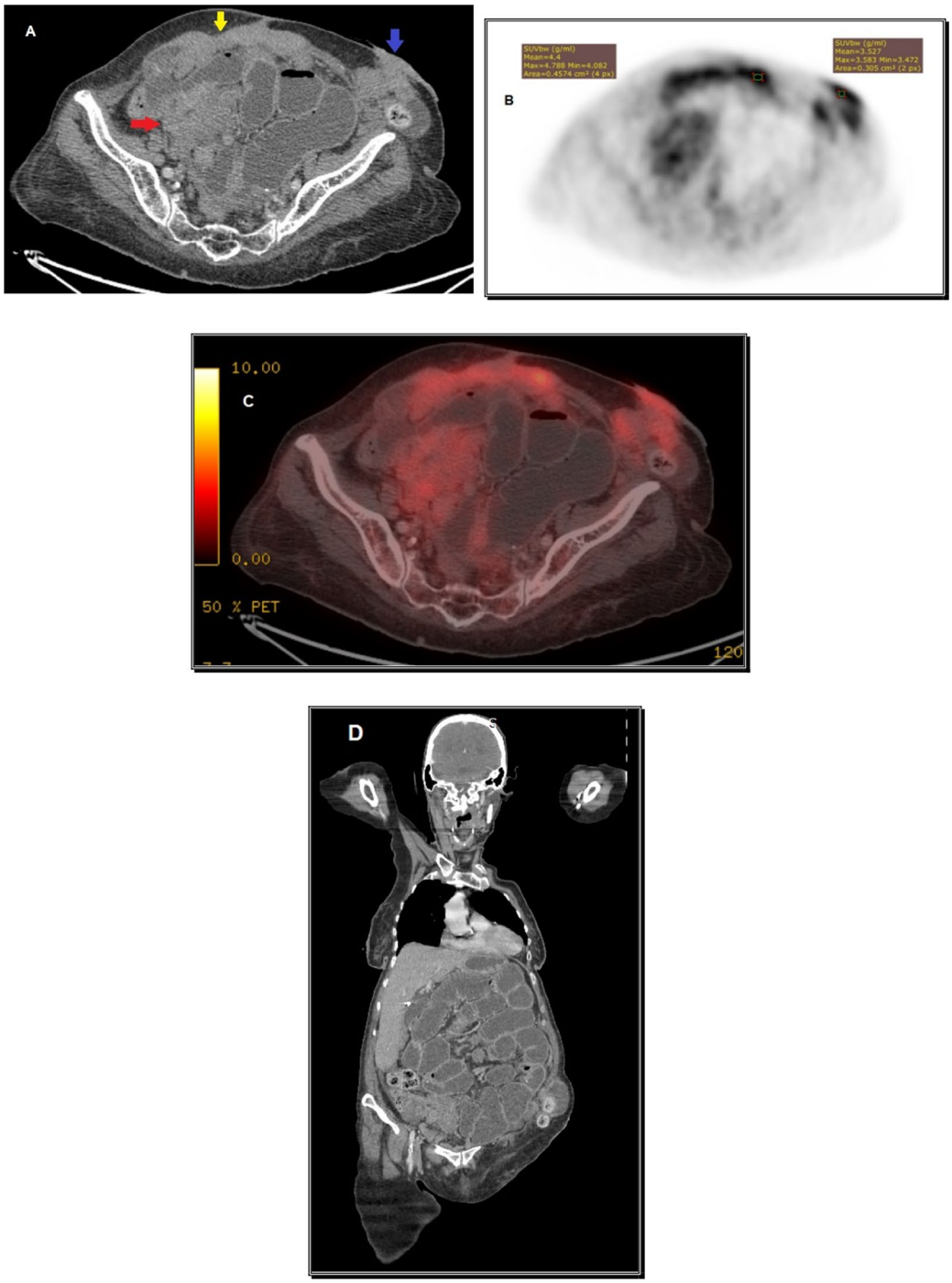

Fig. 7 An 85-year-old female patient with a history of partial colectomy for a colonic mass lesion followed by colostomy. Histopathology revealed colonic adenocarcinoma. Referred for whole body survey **A** Axial contrast-enhanced CT. **B** Axial PET slice at the same level. **C** Corresponding axial fused PET/CT image, status post-operative hemicolectomy and left iliac fossa colostomy showing metabolically active ill-defined lobulated soft tissue lesion related to the medial aspect of the colostomy opening (blue arrow) with smudging of the surrounding fat planes eliciting SUVmax = ~3.5 of focal nodular uptake pattern. Diffuse metabolically active peritoneal thickening, nodularity and soft tissue masses with variable sizes and shapes showing intra-muscular infiltrative lesions along anterior abdominal wall muscles and the subcutaneous fat (yellow arrow), a similar lesion is in the right lumbar region (red arrow) showing focal nodular up take with SUVmax = ~4.7. Dilated bowel loops with air-fluid level, impressive of intestinal obstruction. **D** Coronal contrast-enhanced CT demonstrating the left colostomy, the right lumbar region peritoneal mass and the dilated bowel loops as a complication of peritoneal metastasis

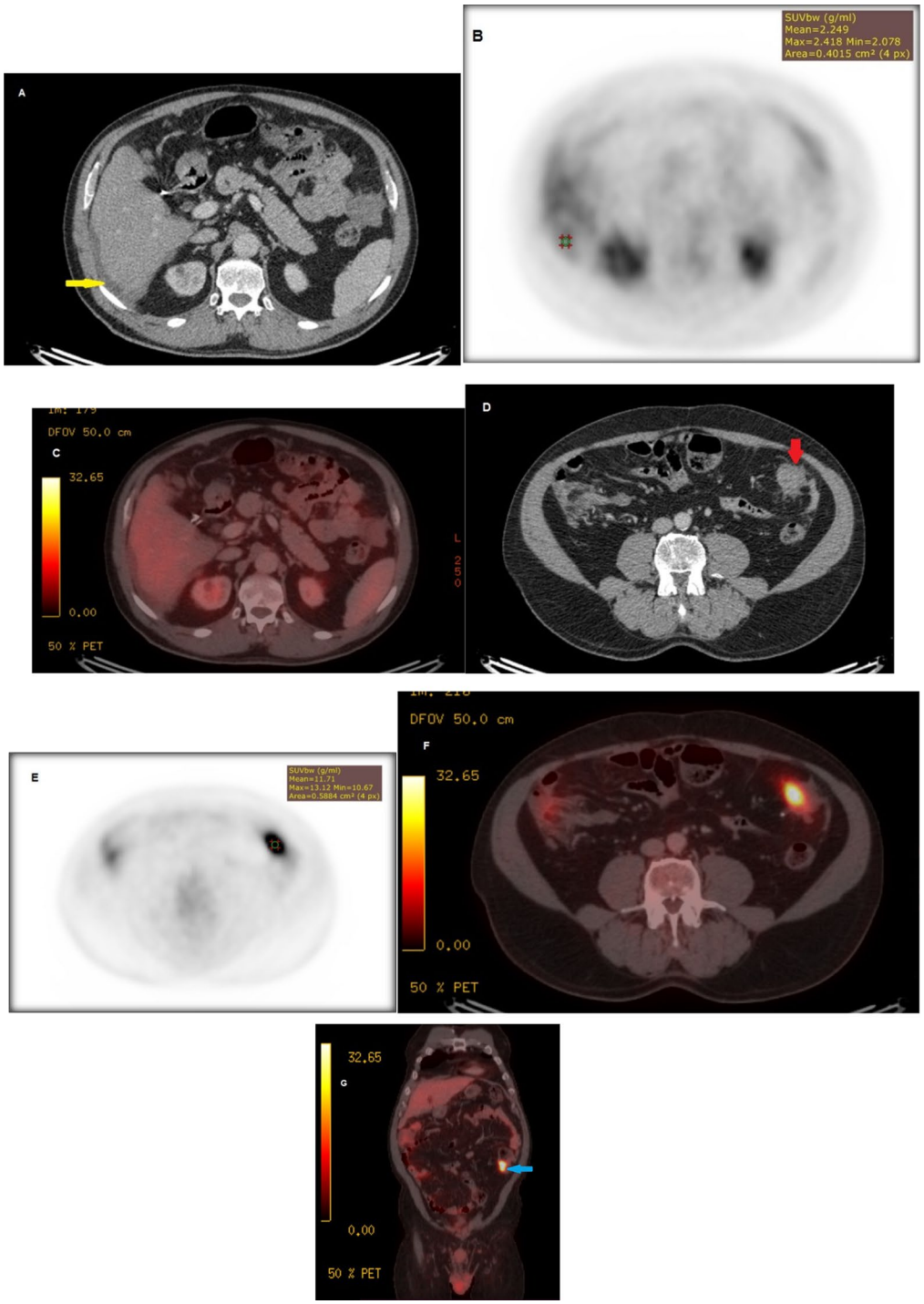

Fig. 8 A 68-year-old male patient with a history of colonic carcinoma under chemotherapy pathologically proved low-grade mucinoid adenocarcinoma, referred for follow-up. **A** Axial contrast-enhanced CT. **B** Axial PET slice at the same level. **C** Corresponding axial fused PET/CT image, showing peritoneal sheets and thickening seen along hepatic peritoneal surfaces scalloping its outline (yellow arrow) with low FDG uptake SUVmax = ~ 2.4. Also, few scattered small nodules in the abdominal cavity underneath the anterior abdominal wall, inseparable from underlying small and large bowel loops of low FDG uptake. **D** Axial contrast-enhanced CT. **E** Axial PET slice at the same level. **F** Corresponding axial fused PET/CT image, showing irregular mural thickening of the distal part of the descending colon with focal soft tissue mass formation (red arrow) with intense metabolic activity eliciting SUVmax = ~ 13. **G** Coronal PET/CT image demonstrating increased activity of the descending colon mass lesion (blue arrow) with low activity of the peritoneal deposits on the liver serosal surfaces

Abbreviations

IV	Intravenously
MUP	Metastasis of unknown primary
NPV	Negative predictive value
PC	Peritoneal carcinomatosis
PET/CT	Positron emission tomography/computed tomography
PPV	Positive predictive value
ROC	Receiver operating characteristic
ROI	Regions of interest
SUV	Standard uptake value

Acknowledgements
Special thanks to our colleagues and seniors in the hospital for their help.

Author contributions
ES suggested the research idea, ensured the original figures and data in the work, minimized the obstacles to the team of work, correlated the study concept and design, and had the major role in analysis. AD collected data in all stages of manuscript, performed data analysis. MD supervised the study with significant contributions to design the methodology, manuscript revision and preparation. AB correlated the clinical data of patient and matched it with the findings, drafted and revised the work. All authors read and approved the final manuscript for submission.

Funding
Not applicable.

Availability of data and materials
The datasets used and/or analysed during the current study are available from the corresponding author on reasonable request.

Declarations

Ethics approval and consent to participate
This study was approved by the ethics committee of Tanta University Hospital. Ethics committee reference numbers is 34312/12/20. Approval of the Research Ethics Committee and written consent were obtained from all participants in the study. Privacy of all patient data was guaranteed.

Consent for publication
The patients provided written consent, and the ethics committee approved this procedure as it suits this research project.

Competing interests
The authors declare that they have no competing interests.

Received: 4 August 2022 Accepted: 6 January 2023
Published online: 17 January 2023

References

1. Patel CM, Sahdev A, Reznek RH (2011) CT, MRI and PET imaging in peritoneal malignancy. Cancer Imaging 11(1):123
2. Wang W, Tan GH, Chia CS, Skanthakumar T, Soo KC, Teo MC (2018) Are positron emission tomography-computed tomography (PET-CT) scans useful in preoperative assessment of patients with peritoneal disease before cytoreductive surgery (CRS) and hyperthermic intraperitoneal chemotherapy (HIPEC)? Int J Hyperthermia 34(5):524–531
3. Dawson H, Kirsch R, Messenger D, Driman D (2019) A review of current challenges in colorectal cancer reporting. Arch Pathol Lab Med 143(7):869–882
4. Pai RR, Shenoy KD, Minal J, Suresh PK, Chakraborti S, Lobo FD (2019) Use of the term atypical cells in the reporting of ascitic fluid cytology: a caveat. CytoJournal 16:13
5. Elekonawo FM, Starremans B, Laurens ST, Bremers AJ, de Wilt JH, Heijmen L, de Geus-Oei LF (2020) Can [18F] F-FDG PET/CT be used to assess the pre-operative extent of peritoneal carcinomatosis in patients with colorectal cancer? Abdom Radiol 45(2):301–306
6. Pletcher E, Gleeson E, Labow D (2020) Peritoneal cancers and hyperthermic intraperitoneal chemotherapy. Surg Clin 100(3):589–613
7. Van't Sant I, Engbersen MP, Bhairosing PA, Lambregts DM, Beets-Tan RG, van Driel WJ, Aalbers AG, Kok NF, Lahaye MJ (2020) Diagnostic performance of imaging for the detection of peritoneal metastases: a meta-analysis. Eur Radiol 30(6):3101–3112
8. Soussan M, Des Guetz G, Barrau V, Aflalo-Hazan V, Pop G, Mehanna Z, Rust E, Aparicio T, Douard R, Benamouzig R (2012) Comparison of FDG-PET/CT and MR with diffusion-weighted imaging for assessing peritoneal carcinomatosis from gastrointestinal malignancy. Eur Radiol 22(7):1479–1487
9. Suzuki A, Kawano T, Takahashi N, Lee J, Nakagami Y, Miyagi E, Hirahara F, Togo S, Shimada H, Inoue T (2004) Value of 18F-FDG PET in the detection of peritoneal carcinomatosis. Eur J Nucl Med Mol Imaging 31(10):1413–1420
10. Funicelli L, Travaini L, Landoni F, Trifirò G, Bonello L, Bellomi M (2010) Peritoneal carcinomatosis from ovarian cancer: the role of CT and [18F] FDG-PET/CT. Abdom Imaging 35(6):701–707
11. Campos NM, Almeida V, CurvoSemedo L (2022) Peritoneal disease: key imaging findings that help in the differential diagnosis. Br J Radiol 95(1130):20210346

Publisher's Note